Electron-spin-resonance studies of the hole-doping effect on $(Tl_{0.5}Pb_{0.5})Sr_2(Ca_{1-x}Y_x)Cu_2O_7$ high-T_c superconductors

Li Yeat Chen and Juh Tzeng Lue
Department of Physics, National Tsing Hua University, Hsinchu, Taiwan, Republic of China

R. S. Liu
Materials Research Laboratories, Industrial Technology Research Institute, Hsinchu, Taiwan, Republic of China
(Received 2 May 1995; revised manuscript received 18 July 1995)

In this work, we attempt to investigate the relation between the hole-doping effect and electron spin resonance (ESR) spectra in the series of $(Tl_{0.5}Pb_{0.5})Sr_2(Ca_{1-x}Y_x)Cu_2O_7$ high-T_c superconductors. The spin signal is absent for $x=0.2$ which is the optimal doping for obtaining a maximum T_c, while the ESR signals recover for the underdoped and overdoped samples. This result can be expressed by the slowing down of the superexchange force between next-neighboring copper ions which retrieve their native local moments by the increase or decrease of hole doping. The unexpected vanish of ESR spectra for the antiferromagnetic insulator at $x=0.9$ implicates a highly correlated spin fluctuation in the $(Tl_{0.5}Pb_{0.5})Sr_2(Ca_{1-x}Y_x)Cu_2O_7$ system.

I. INTRODUCTION

Since the discovery of cuprate superconductors, the absence of an electron spin resonance (ESR) signal in their normal state is still a conjecture.[1-3] Many experiments, e.g., neutron diffraction,[4] nuclear magnetic resonance (NMR),[5] photoemission,[6] etc., indirectly support that these cuprate compounds and their insulating antiferromagnetic derivatives are divalently coupled within the CuO_2 planes by the Heisenberg exchange field. However, the electron spin resonance signal derived from paramagnetic Cu^{2+} ions was not observed in high-T_c cuprate superconductors such as $La_{1.85}Sr_{0.15}CuO_4$, $YBa_2Cu_3O_{7-\delta}$, and Bi- and Tl(2212)-based systems.[7] The null spin evidence had been interpreted by several theories including Anderson's resonating valence bond (RVB) theory[8] and anyon superconductivity.[9] Some authors attribute their detected ESR signals by the contribution from the minor phase,[1] localized electron spins in copper ions,[2] and the broken cubic symmetry in copper-oxide chains.[10] One of the most interesting features exhibited in the $GdBa_2Cu_3O_7$ compound is that it shows a very strong spin signal due to the presence of paramagnetic Gd^{3+} ions.[11]

In previous studies of the $YBa_2Cu_3O_{7-\delta}$ system,[12,13] we pointed out that the spins of two neighboring Cu^{2+} ions can flip-flop through intermediate oxygen atoms. The hopping integral between the vibronic wave functions of the distorted structure may occur more rapidly between the states of opposite spins than between the Kramers conjugates and provide a plausible mechanism for an enhanced exchange force. If the ESR probing frequency is far smaller than the exchange frequency $J/\hbar$ ($\sim 1.5\times 10^{13}$ Hz), then the detecting system will observe an average spin $S=0$, although spontaneously it is an antiferromagnetic state with very fast exchange of spin up and down between the neighboring Cu^{2+} paramagnetic ions, and no ESR signal can be detected in the highest superconducting phase. The deficiency of oxygen atoms in this compound will degrade the doping effect and slow down the superexchange rate. Thus the singlet pairing state will be spoiled, yielding local moments. There are still some questions about the role of spins under the influence of hole doping in the copper-oxygen planes.

In this work, the controllable metal-superconductor-insulator transition by the chemical substitution of Y^{3+} for Ca^{2+} in $(Tl_{0.5}Pb_{0.5})Sr_2(Ca_{1-x}Y_x)Cu_2O_7$ in order to reduce the hole concentration in the conducting CuO_2 planes has been investigated. When the doping concentration is $x=0.2$, which we defined as the optimal hole concentration in the CuO_2 planes, the ESR signal vanishes, which corresponds to a highest T_c. Samples in the underdoped or overdoped region, however, will enhance the ESR signal and decrease the T_c. Thus, as we previously proposed,[12] the coupling of hole spins by the suppression of the superexchange interaction $J=-t^2/u$ where t is the hopping integral and u is the effective Hubbard on-site interelectronic Coulomb repulsion due to underdoping or overdoping, leads to the retrieving of the original local moments of the copper ions.

II. SAMPLE CHARACTERISTICS

Samples with nominal compositions of $(Tl_{0.5}Pb_{0.5})Sr_2(Ca_{1-x}Y_x)Cu_2O_7$ were prepared by an appropriate stoichiometric proportions of high-purity $CaCO_3$, Y_2O_3, $SrCO_3$, and CuO compounds and calcined at 970 °C for 12 h in air to form a precursor. The precursor was then mixed with Tl_2O_3 and PbO, ground, and pressed into cylindrical pellets under a pressure of 2 ton/cm^2. The pellets were wrapped in gold foils to prevent the loss of Tl and Pb during heating. The samples were then sintered at 950 °C for 3 h in flowing oxygen, followed by cooling to room temperature at a rate of 5 °C/min.

Based on the previous results,[14] the critical temperatures and hole numbers distributed to each copper ion of the samples $(Tl_{0.5}Pb_{0.5})Sr_2(Ca_{1-x}Y_x)Cu_2O_7$ for various values of x determined from the resistivity and Hall constant measurements are listed in Table I. We can classify the doping into three regions: the overdoped region for $0\leq x<0.2$, the optimum region for $x=0.2$, and the underdoped region for

TABLE I. T_c and hole numbers per Cu atom of $(Tl_{0.5}Pb_{0.5})Sr_2(Ca_{1-x}Y_x)Cu_2O_7$ (Ref. 14).

x	0.0	0.1	0.2	0.3	0.4	0.5	0.9
T_c (K)	73	98	106	100	85	42	
Hole number/Cu	0.48	0.36	0.2	0.14	0.12	0.06	

$0.2<x\leq 1$. As the value of x approaches 0.6, it is almost located at the metal-insulator phase boundary. Based on neutron- and x-ray-diffraction studies,[14] the crystal structure of $(Tl_{0.5}Pb_{0.5})Sr_2(Ca_{1-x}Y_x)Cu_2O_7$ can be determined as shown in Fig. 1(a). The structure can be described in terms of an intergrowth of double rocksalt-type layers [({Tl/Pb}O)(SrO)] with double $[Sr(Ca,Y)Cu_2O_5]$ oxygen-deficient perovskite layers, formed by sheets of corner-sharing CuO_5 pyramids interleaved with calcium and/or yttrium ions. The structure of $(Tl_{0.5}Pb_{0.5})Sr_2(Ca_{1-x}Y_x)Cu_2O_7$ resembles that of $YBa_2Cu_3O_7$ [as shown in Fig. 1(b)] where the (Tl,Pb)-O layers replace the Cu-O chains and Sr cations replace Ba cations, and Ca cations partially substitute yttrium ions. However, there is no significant variation of the oxygen content in the $(Tl_{0.5}Pb_{0.5})Sr_2(Ca_{1-x}Y_x)Cu_2O_7$ series compounds when the Y^{3+} ions substitute into the Ca^{2+} sites, as determined by neutron-diffraction measurements.[14] According to the results of various measurements[14] (e.g., neutron diffraction, resistivity, Hall effect, and thermoelectric power, etc.), the increase of the substitution concentration of Y^{3+} for the Ca^{2+} ions implies several results: (1) elongation of Cu-O bond lengths in the copper-oxygen plane, (2) increasing of the room temperature resistivity, (3) decreasing of the effective number of holes in the conducting CuO_2 planes, and (4) increasing of the absolute value of the thermoelectric power.

III. EXPERIMENTAL RESULTS

A microcomputer-controlled Phillips diffractometer x-ray equipped with a copper target and graphite monochromator for Cu$K\alpha$ radiation was used to obtain the powder x-ray-diffraction (XRD) patterns. All the samples of $(Tl_{0.5}Pb_{0.5})Sr_2(Ca_{1-x}Y_x)Cu_2O_7$ $(0\leq x\leq 1)$ are monophase according to the P4/mmm space group. In Fig. 2, we show a typical XRD pattern of the $x=0.3$ sample, which can be indexed on the basis of a tetragonal unit cell having $a=3.810(1)$ Å and $c=12.066(2)$ Å.

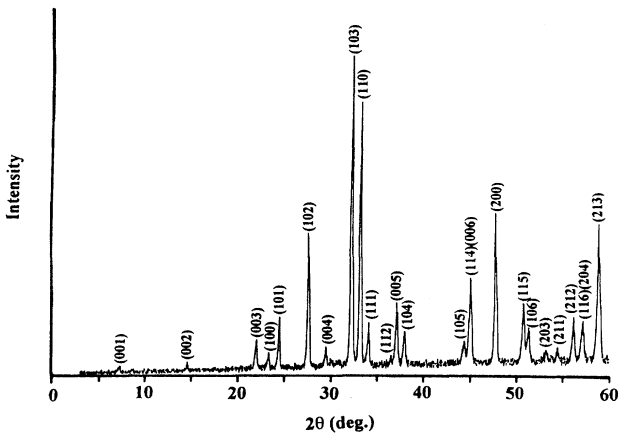

FIG. 2. Typical XRD pattern of the $x=0.3$ sample in $(Tl_{0.5}Pb_{0.5})Sr_2(Ca_{1-x}Y_x)Cu_2O_7$.

Field cooled ($H=10$ Oe) magnetization data (the Meissner effect) were obtained using a superconducting quantum interference device (SQUID) magnetometer (Quantum Design). In Fig. 3, we show the temperature dependence of the field-cooled magnetization of the $(Tl_{0.5}Pb_{0.5})Sr_2(Ca_{1-x}Y_x)Cu_2O_7$ $(0\leq x\leq 1)$ powdered samples. With increasing the x values, the diamagnetism onset temperature increases from 73 K for $x=0$ to a maximum of 106 K for $x=0.2$ and then decreases. We therefore can identify three regions by the variation of the hole concentration: (a) the overdoped region $(0\leq x<0.2)$, (b) the optimal region $(x=0.2)$, and (c) the underdoped region $(0.2<x\leq 1)$.

The ESR spectra were measured by employing a Brucker GmbH-type ER-200 spectrometer with a TE_{104} double rectangular cavity at a microwave frequency of 9.56 GHz and a modulation frequency of 100 kc/s. Figure 4 shows the ESR signals for different compositions. The doping at $x=0$ induces a maximum hole density, and the spectrum reveals a broad linewidth. Increasing x to 0.2, the optimum doping for obtaining the maximum T_c, the ESR spin signal disappears, while the ESR reappears as x increases, and the intensity

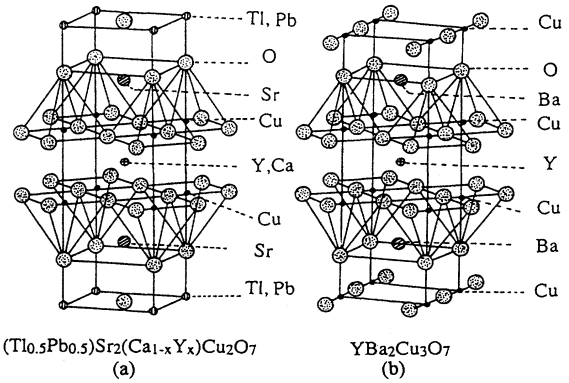

FIG. 1. Representation of the crystal structures of (a) $(Tl_{0.5}Pb_{0.5})Sr_2(Ca_{1-x}Y_x)Cu_2$-$O_7$ and (b) $YBa_2Cu_3O_7$.

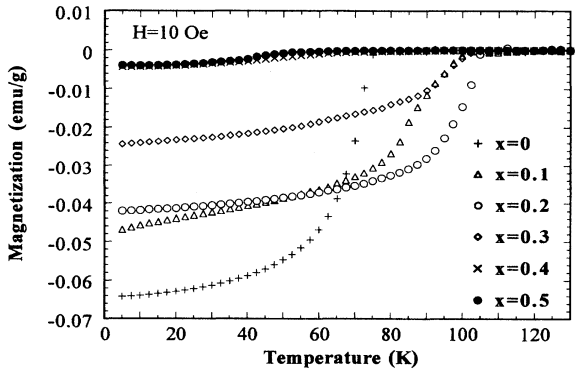

FIG. 3. Temperature dependence of the field-cooled magnetization of the powdered $(Tl_{0.5}Pb_{0.5})Sr_2(Ca_{1-x}Y_x)Cu_2O_7$ $(0\leq x\leq 0.5)$ samples.

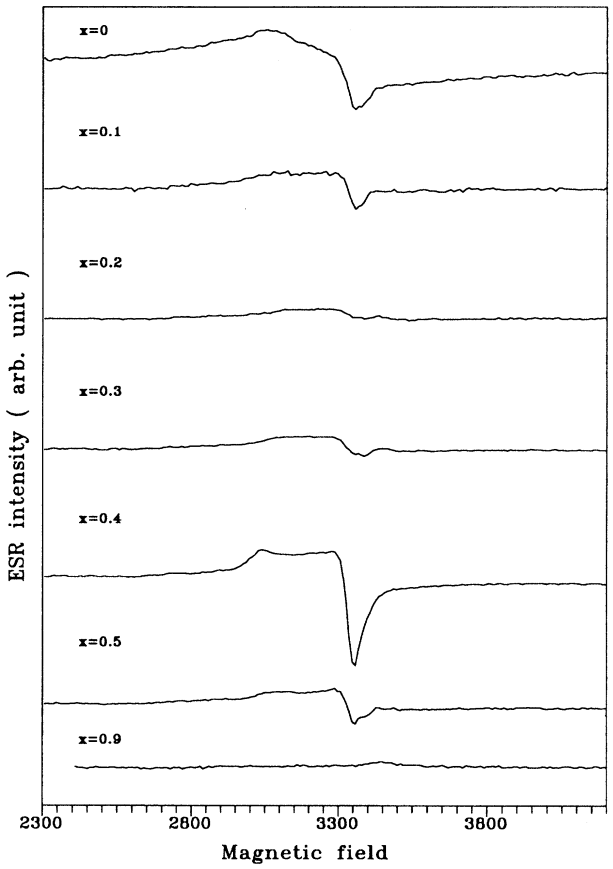

FIG. 4. ESR spectra for various x values of $(Tl_{0.5}Pb_{0.5})Sr_2(Ca_{1-x}Y_x)Cu_2O_7$ superconductors. Note that $x=0.9$ is an antiferromagnetic phase without superconductivity.

approaches a maximum for $x=0.4$. When $x=0.5$, the signal decreases rapidly. All the intensities of the spectra with different values of x were calibrated in the scale of the diphenyl picrylhydrazyl (DPPH) signal. In the overdoped condition ($0\leq x<0.2$), the increase of the hole spin intensity results in a weakening of the superexchange interaction and producing a higher antiferromagnetic background which has a rather broad line. On the other hand, in the underdoped condition ($0.2<x\leq 1$), the low hole spin density not only suppresses the antiferromagnetic background, but also reduces the superexchange force in the copper-oxide planes. In this region, the local moments of copper ions have strong hyperfine interaction field to contribute to the ESR signal which has a narrow linewidth. It is worth noting that the measurement of the thermal electric power for the $x=0$ sample shows a negative value and the specific heat tends to exhibit a high spin density.[14] However, when the value of x attains 0.9, implying an antiferromagnetic phase, the ESR signal disappears again. We tacitly assume that the strong magnetic dipole-dipole broadening overwhelms the exchange narrowing of the antiferromagnetic phase at $x=0.9$ and smears out the ESR signal.

IV. THEORETICAL ANALYSIS

Comparing with the structure of $YBa_2Cu_3O_7$ (as shown in Fig. 1), there is no Cu-O chain in the $(Tl_{0.5}Pb_{0.5})Sr_2(Ca_{1-x}Y_x)Cu_2O_7$ superconductors, informing the diminishing of the tunneling of spins between neighboring copper ions. The copper Cu^{2+} ions are strongly paramagnetic with a nuclear spin of $I=\frac{3}{2}$. The same method utilized in Ref. 15 to calculate the ESR spectra based on copper ingredients can also be applied to the $(Tl_{0.5}Pb_{0.5})Sr_2(Ca_{1-x}Y_x)Cu_2O_7$ system. The spin-orbit interaction $\lambda l\cdot s$ can admix the ground state, $Cu^{2+}:d_{x^2-y^2}$, into the excited state and yield an anisotropic g factor. The spin Hamiltonian can be written as

$$H=g_{\parallel}\beta S_z H_z+g_{\perp}(S_x H_x+S_y H_y)+A_{\perp}(S_x I_x+S_y I_y)+\lambda l\cdot s, \tag{1}$$

where the Lande g values parallel and perpendicular to the z axis are $g_{\parallel}=2(1+4\lambda/\Delta_0)$ and $g_{\perp}=2(1+\lambda/\Delta_1)$, respectively, Δ_0 and Δ_1 are the energy differences between the ground $|x^2-y^2\rangle$ and the excited $|xy\rangle$, $|yz\rangle$, and $|zx\rangle$ states, respectively, and the $A_{\parallel}$ and $A_{\perp}$ are the contact hyperfine constants with nuclear spin I. The magnetic field at resonance for the hyperfine line M_I calculated by second-order perturbation is[16]

$$H=H_0-\frac{KM_I}{g\beta}-\frac{A_{\perp}^2(A_{\parallel}^2+K^2)[I(I+1)-M_I^2]}{4H_0(g\beta K)^2}$$
$$-\frac{A_{\perp}^2A_{\parallel}(2m_s-1)M_I}{2(g\beta)^2K}-\frac{(A_{\parallel}^2-A_{\perp}^2)^2g_{\parallel}^2g_{\perp}^2z^2(1-z^2)M_I^2}{2H_0(g\beta)^2K^2g^4}, \tag{2}$$

where $H_0=h\nu/g\beta$, $g^2=g_{\perp}^2+(g_{\parallel}^2-g_{\perp}^2)z^2$, $K^2g^2=A_{\parallel}^2g_{\parallel}z^2+A_{\perp}^2g_{\perp}^2(1-z^2)$, $z=\cos\theta$, and $M_I=\pm\frac{1}{2},\pm\frac{3}{2}$.

The derivative line shape of the absorption curve at the applied field H_a is

$$I(H_a)=\frac{g_{\perp}^2}{8(2I+1)}\int_0^1 S'(H-H_a)\left[\left(\frac{g_{\parallel}}{g_{\perp}}\right)^2+1\right]dz, \tag{3}$$

where $S'(x)$ for a normalized Lorentz line shape is given by

$$S'(x)=\frac{2x}{\pi\alpha^3[1+(x/\alpha)^2]^2},$$
$$\alpha=\frac{\sqrt{3}\Delta H}{2}, \tag{4}$$

at which the ΔH is the full width at half maximum (FWHM) of the absorption line. For a large value of ΔH, the four hyperfine lines will be merged into two asymmetric lines.

In order to analyze the difference between underdoped and overdoped $(Tl_{0.5}Pb_{0.5})Sr_2(Ca_{1-x}Y_x)Cu_2O_7$ samples, we compare the spectra of the $x=0$ (overdoped) and $x=0.4$ (underdoped samples. The spectra are simulated by five parameters, i.e., $g_{\parallel}$, $g_{\perp}$, $A_{\parallel}$, $A_{\perp}$, and ΔH, which are derived by a tedious curve fitting. The curve fitting for the sample with $x=0$ is shown in Figs. 5(a) and 5(b). We assumed that there are two spins due to different locations of Tl,Pb sites corresponding to two sets of fitting parameters because the arrangement of Tl/Pb atoms is either parallel or orthogonal with each other in the $(Tl_{0.5}Pb_{0.5})$-O plane as shown in Fig. 1. Thus a half unit cell of $(Tl_{0.5}Pb_{0.5})Sr_2(Ca_{1-x}Y_x)Cu_2O_7$ can be represented by one kind of spin corresponding to

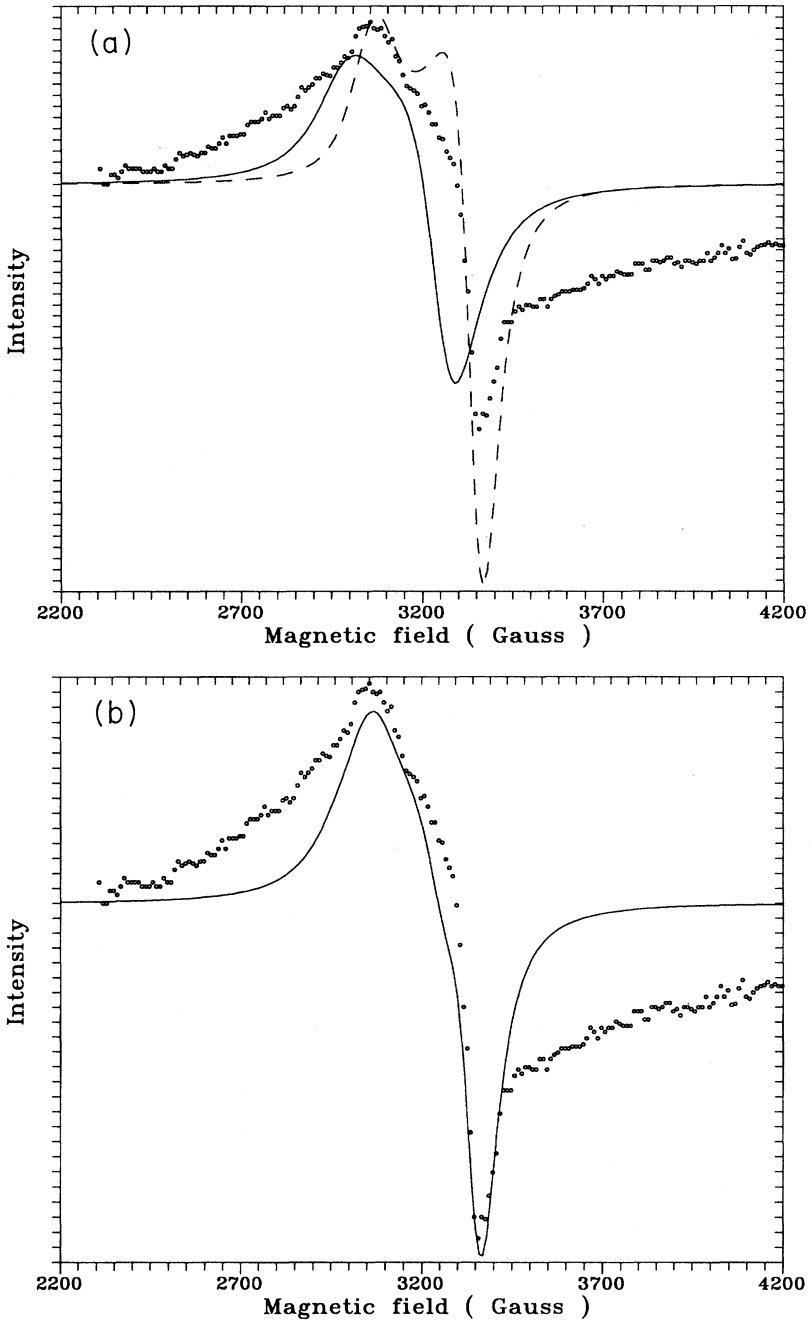

FIG. 5. (a) Two spin states are used to fit the ESR line shape for $x=0$ sample with fitting parameters given by (1) dashed line: $g_{\parallel}=2.161$, $g_{\perp}=1.98$, $A_{\parallel}=21.0$, $A_{\perp}=10.3$, $\Delta H=70$ G; and (2) solid line: $g_{\parallel}=2.211$, $g_{\perp}=2.03$, $A_{\parallel}=21.0$, $A_{\perp}=10.3$, $\Delta H=120$ G. (b) Addend (solid line) of the above two lines as compared with the experimental curve (dotted line).

copper ions located in cells with different Tl or Pb atoms. They are (a) $g_{\parallel}=2.161$, $g_{\perp}=1.98$, $A_{\parallel}=21.0$, $A_{\perp}=10.3$, $\Delta H=70$ G and (b) $g_{\parallel}=2.211$, $g_{\perp}=2.03$, $A_{\parallel}=21.0$, $A_{\perp}=10.3$, $\Delta H=120$ G, respectively. Comparing with the theoretical curve for a pure hyperfine interaction of a single spin, the highly asymmetric ESR curve might be extracted from the antiferromagnetic resonance background. Such an antiferromagnetic lattice structure in high-T_c superconductors has been presumed to be an important clue to mediate the electron pairing mechanism.[17] To justify Anderson's arguments, the doping might transform the antiferromagnetic states into the resonating valence bond states in which the spin polarities of neighboring coppers are quickly exchanged. The variation of magnetic field for an antiferromagnetic resonance (AFMR) can be expressed as[18,19]

$$H=H_0\pm[H_A(2H_E+H_A)]^{1/2}, \tag{5}$$

where H_E and H_A are the exchange and anisotropic fields, respectively. As shown in Fig. 6, we assume two antiferromagnetic states belonging to two different sites of the spin with $H_0=3160$ and 3310 G, respectively. The line shapes of the AFMR are presumed to be Lorentzian with parameters $g=2.048$, $H_E=126.6$ G, and $H_A=21.3$ G and linewidth

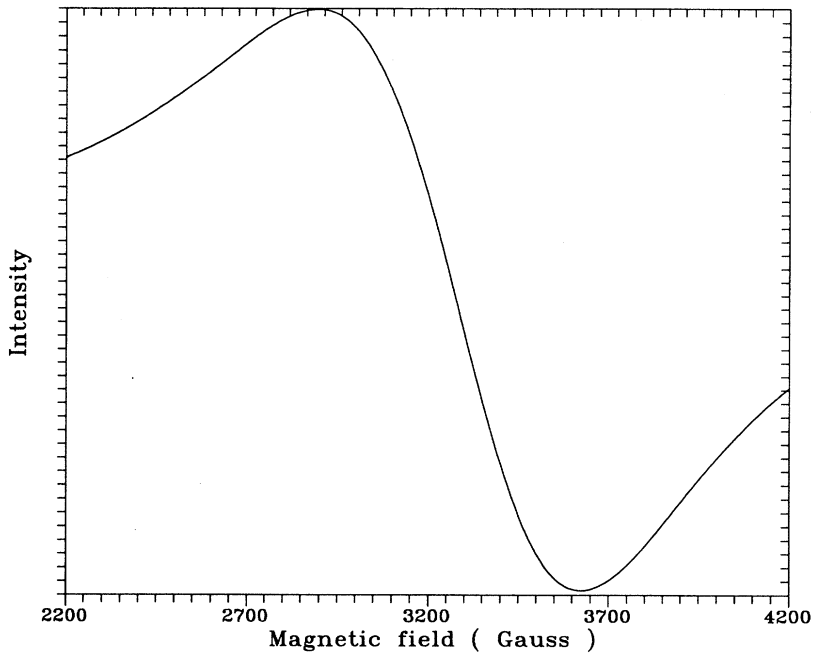

FIG. 6. Spectrum showing the antiferromagnetic background, where the two resonant magnetic fields are $H_0 = 3160$ and 3310 G, and the Lorentzian linewidth is 720 G.

$\Delta H = 720$ G. The summation of the hyperfine lines (Fig. 5) and the antiferromagnetic resonance lines (Fig. 6) can fairly match the experimental data for $x = 0$ as depicted in Fig. 7. Concerning the system with $x = 0.4$, the simple summation of four sets of hyperfine lines can almost fit the data as shown in Fig. 8. The four hyperfine constants arise from the unequivalent Ca or Y substitutes. Figure 9 shows the correction with the AFMR for the $x = 0.4$ sample. The contributions of the AFMR to the fitting curves for the $x = 0$ and $x = 0.4$ samples are 51.5% and 10.1%, respectively. The decrease of the contribution of the AFMR to the ESR intensity as x increases from 0 to 0.4 may be correlated to the increase of the superconducting volume fraction (proportional to the value of the magnetization). In practice, the AFMR spectrum detected by the X-band microwave under a magnetic field of thousands of oersterd is weak and has a broad linewidth. Therefore, the shoulder at low-field side for the $x = 0$ sample might come from the AFMR.

From the above analysis, the hyperfine interaction constant of Cu^{2+} ions in overdoped samples is weaker than in underdoped samples. The origins of the two antiparallel spins come mainly from a weakening of the superexchange force which leads to a retrieval of their local moments. The strong polarization effect of Tl atoms on the anion inducing

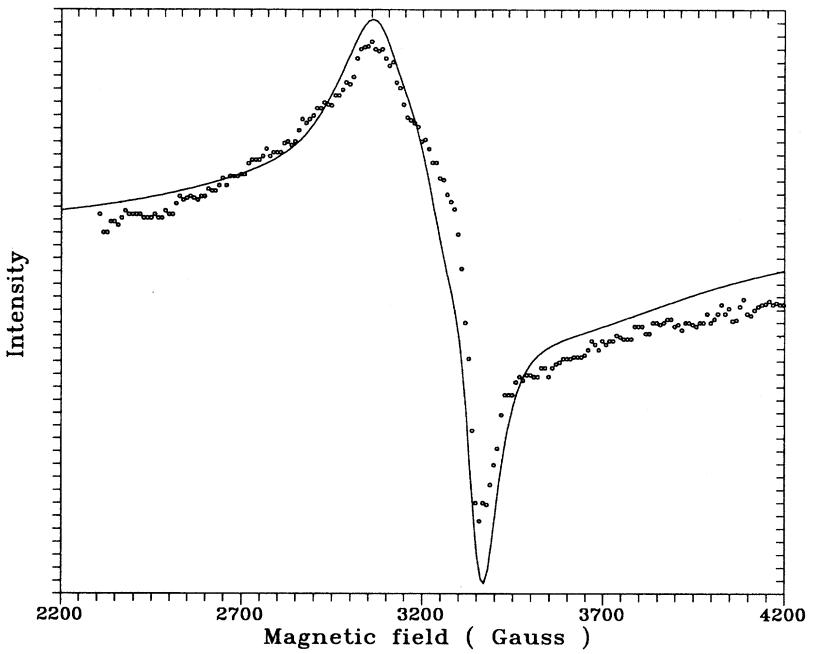

FIG. 7. Solid line is the correction by the antiferromagnetic background for the $x = 0$ sample.

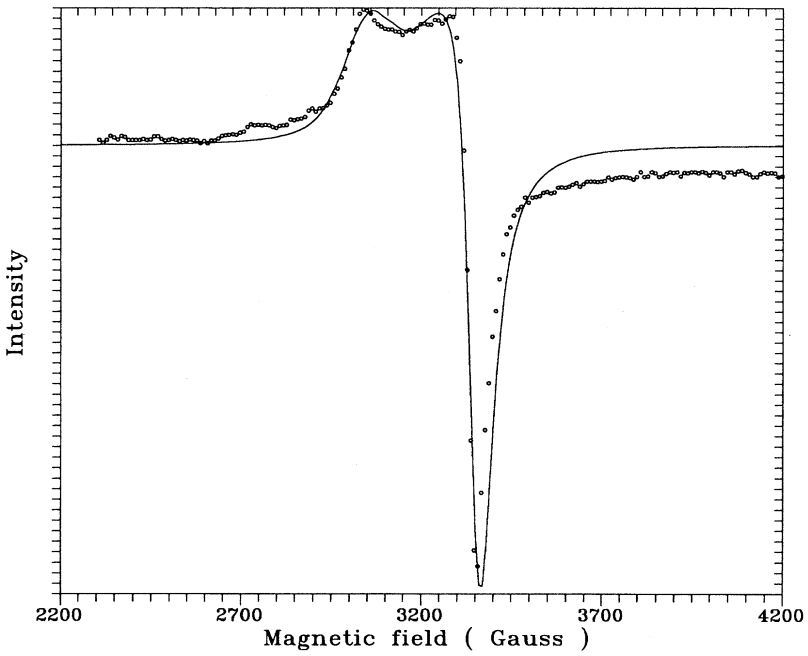

FIG. 8. Addend (solid line) of the above four lines as compared with experimental data for $x=0.4$. The fitting parameters of the four spins for $x=0.4$ sample are (1) $g_{\parallel}=2.181$, $g_{\perp}=1.98$, $A_{\parallel}=51.0$, $A_{\perp}=10.3$, and $\Delta H=50$ G. (2) $g_{\parallel}=2.151$, $g_{\perp}=1.98$, $A_{\parallel}=21.0$, $A_{\perp}=10.3$, and $\Delta H=100$ G, (3) $g_{\parallel}=2.181$, $g_{\perp}=1.98$, $A_{\parallel}=21.0$, $A_{\perp}=10.3$, and $\Delta H=50$ G, and (4) $g_{\parallel}=2.111$, $g_{\perp}=2.01$, $A_{\parallel}=81.0$, $A_{\perp}=10.3$, and $\Delta H=95$ G.

the phonon vibration modes of the conducting Cu-O planes will increase the density of states near the Fermi surface and enhance the Josephson microtunneling between Cu-O planes.[20] A theory concerning the cyclic four spins of the copper-oxide plane had been reported;[21,22] however, the hyperfine splitting of four spins on Cu-O planes in our underdoped or overdoped cases cannot be found as the authors showed in the case of CuO. It is very interesting to note that the $x=0.2$ sample is superconducting, while that the $x=0.9$ sample is antiferromagnetic, but both have no ESR signal. Since antiferromagnetic spin fluctuations play an important role in cuprate superconductor,[23] the $x=0.2$ sample seems to have highly correlated electron spins, which flip-flop rapidly in the normal state. Such an antiferromagnetic spin fluctuation provides a mediating force to pair the conduction electrons at rather high temperatures. The energy of antiferromagnetic paramagnon, ω_{SF}, characterizing the energy of the low-frequency magnetic response, is about 7.7 meV (i.e., ~ 1860 GHz) at T_c as measured for the nuclear magnetic resonance (NMR) study.[24,25] Therefore, an ESR system at a probing frequency of 9 GHz is unable to detect the fast exchange spin states. Once the doping increases or decreases from $x=0.2$, the highly correlated spins become unbalanced due to the reduction of superexchange rate and the ESR sig-

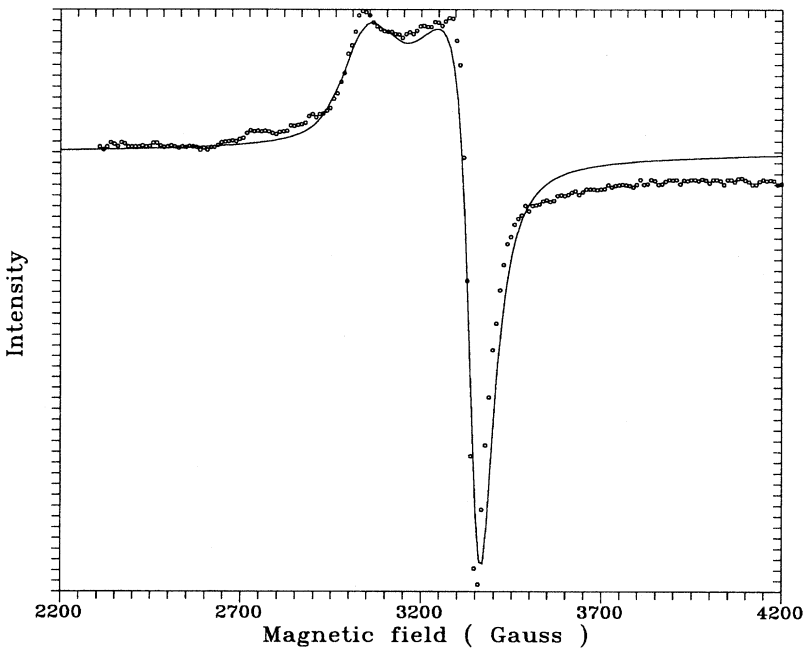

FIG. 9. Contribution of AFMR for the $x=0.4$ sample is reduced much more than that for the $x=0$ sample.

nal appears at both overdoped and underdoped regions. When x varies from 0.5 to 0.9, the sample transforms to antiferromagnetic phase, and the strong dipole-dipole broadening smears out the ESR signal. The calculation of carrier concentrations for $YBa_2Cu_3O_7$ by Monthoux and Pines[25] pointed out that the decrease of hole number will reduce the T_c at a fixed coupling constant. However, for the $(Tl_{0.5}Pb_{0.5})Sr_2(Ca_{1-x}Y_x)Cu_2O_7$ superconductors, which manifest a maximum T_c at $x=0.2$, while the hole number is not at an extreme value, further exploration is needed.[26]

V. CONCLUSION

For the $x=0.2$ sample, the absence of an ESR spin signal is attributed to the quick spin flip-flop inherent to copper ions through the fast superexchange rate between next-neighboring ions, which yields $S=0$ for a comparably stationary observer, implying a diamagnetic state even at $T>T_c$. The slowdown of the spin flip-flop of the antiparallel spins of the overdoped samples evokes a weak antiferromagnetic background and two anisotropic local spin states involving two different g factors and hyperfine constants. The experimental spectra can be successfully fitted by a proper weight mixture of an antiferromagnetic resonance, and the two-site magnetic hyperfine interaction on the antiferromagnetic resonance derives from a static spin system, i.e., the spins corrected to second order. The possibility of the ESR signal arising from impurities is ruled out because all the spectra exhibit similar shapes, and the impurities might be preserved even when the doping concentration is changed. The hole doping which is analogous to the decrease of oxygen atoms near the Cu-O planes in $YBa_2Cu_3O_7$ suppresses the negative charge transfer from copper ions, resulting in a reduction of the superexchange force between the next-neighboring paramagnetic Cu^{2+} ions.

ACKNOWLEDGMENTS

This work was supported by the National Science Council of the Republic of China under Contract No. NSC 84-2112-M007.

[1] D. C. Vier, S. B. Oseroff, C. T. Shalling, J. F. Smyth, S. Schultz, Y. Dalichaouch, B. W. Lee, M. B. Maple, Z. Fisk, and J. D. Thompson, Phys. Rev. B **36**, 8888 (1987).
[2] G. J. Bowden, P. R. Elliston, K. T. Wan, S. X. Dou, K. E. Easterling, A. Bourdillon, C. C. Sorrell, B. A. Cornell, and F. Separovic, J. Phys. C **20**, L545 (1987).
[3] F. Mehran, S. E. Barnes, E. A. Giess, and T. R. McGuire, Solid State Commun. **67**, 55 (1988).
[4] J. M. Tranquada, A. H. Moudden, A. I. Goldman, P. Zolliker, D. E. Cox, G. Shirane, S. K. Sinha, D. Vaknin, D. C. Johnston, M. S. Alvarez, A. J. Jacobson, J. T. Lewandowski, and J M. Newsam, Phys. Rev. B **38**, 2477 (1988).
[5] C. H. Pennington, D. J. Durand, C. P. Slichter, J. P. Rice, E. D Bukowski, and D. M. Ginsberg, Phys. Rev. B **39**, 2902 (1989).
[6] J. A. Yarmoff, D. R. Clarke, W. Drube, U. O. Karlsson, A. Taleb-Ibrahimi, and F. J. Himpsel, Phys. Rev. B **36**, 3967 (1987).
[7] F. Mehran, S. E. Barnes, G. V. Chandrashekhar, T. R. McGuire, and M. W. Shafer, Solid State Commun. **67**, 1187 (1988).
[8] S. Kivelson, Phys. Rev. B **36**, 7237 (1987).
[9] F. Mehran, Phys. Rev. B **46**, 5640 (1992).
[10] F. Mehran, S. E. Barnes, T. R. McGuire, T. R. Dinger, D. L. Kaiser, and Holtzberg, Solid State Commun. **66**, 299 (1988).
[11] F. Mehran, S. E. Barnes, C. C. Tsuei, and T. R. McGuire, Phys. Rev. B **36**, 7266 (1987).
[12] Juh Tzeng Lue, Phys. Rev. B **38**, 4592 (1988).
[13] Juh Tzeng Lue, Cho-Chin Wu, R. S. Liu, J. M. Liang, and P. T. Wu, J. Phys. Chem. Solids **51**, 65 (1990).
[14] R. S. Liu and P. P. Edwards, Mater. Sci. Forum **130-132**, 435 (1993).
[15] S. S. P. Parkin, V. Y. Lee, A. I. Nazzal, R. Savoy, T. C. Huang, G. Gorman, and R. Beyers, Phys. Rev. B **38**, 6531 (1988).
[16] T. Vanngard and R. Aasa, in *Paramagnetic Resonance*, Proceedings of the first international conference held in Jerusalem, edited by W. Low (Academic, New York, 1963), Vol. II, p. 509.
[17] J. T. Lue and P. T. Wu, Solid State Commun. **66**, 55 (1988).
[18] F. Keffer and C. Kittel, Phys. Rev. **85**, 321 (1952).
[19] C. Kittel, Phys. Rev. **82**, 565 (1951).
[20] A. Muller, C. K. Jorgensen, and E. Diemann, Anorg. Allg. Chem. **391**, 38 (1972).
[21] M. Roger and J M. Delrieu, Phys. Rev. B **39**, 2299 (1989).
[22] R. J. Singh, Alex Punnoose, Jilson Mathew, B. P. Maurya, M. Umar, and M. I. Haque, Phys. Rev. B **49**, 1346 (1994).
[23] P. Monthoux and D. Pines, Phys. Rev. B **47**, 6069 (1993).
[24] A. J. Millis, H. Monien, and D. Pines, Phys. Rev. B **42**, 167 (1990).
[25] P. Monthoux and D. Pines, Phys. Rev. B **49**, 4261 (1994).
[26] St. Lenck, J. P. Carbotte, and R. C. Dynes, Phys. Rev. B **49**, 6933 (1994).